



Opinion

Promotion of oxidative phosphorylation by complex I-anchored carbonic anhydrases?

Hans-Peter Braun ^{1,*} and Niklas Klusch ^{2,*}

The mitochondrial NADH-dehydrogenase complex of the respiratory chain, known as complex I, includes a carbonic anhydrase (CA) module attached to its membrane arm on the matrix side in protozoans, algae, and plants. Its physiological role is so far unclear. Recent electron cryo-microscopy (cryo-EM) structures show that the CA module may directly provide protons for translocation across the inner mitochondrial membrane at complex I. CAs can have a central role in adjusting the proton concentration in the mitochondrial matrix. We suggest that CA anchoring in complex I represents the original configuration to secure oxidative phosphorylation (OXPHOS) in the context of early endosymbiosis. After development of ‘modern mitochondria’ with pronounced cristae structures, this anchoring became dispensable, but has been retained in protozoans, algae, and plants.

Mitochondria and oxidative phosphorylation

Mitochondria are known as the powerhouses of the cell [1]. They perform a plethora of functions involving the biosynthesis of phospholipids, amino acid metabolism, biogenesis of **iron–sulfur clusters** (see [Glossary](#)), adjustment of cellular calcium levels, and initiation of cell death programs [2]. However, a dominant role of mitochondria in aerobically living cells is their contribution to cellular respiration. Several features of these organelles resemble those of **Alphaproteobacteria**, which suggests that the origin of mitochondria derived from endocytosis 1 to 2 billion years ago [3,4]. This theory is based on numerous molecular and cellular features, including the fact that mitochondria have an outer and inner membrane resembling those of Alphaproteobacteria. The porous outer membrane forms an envelope around the mitochondria and separates the organelles from the **cytosol** of the cell. Different protein complexes and channels in this membrane allow the free passage of ions and small organic compounds. By contrast, the inner membrane forms a selectively permeable barrier. Together, the outer and inner mitochondrial membrane divide the organelles into different compartments. The so-called ‘**intermembrane space**’ is the outermost compartment and lies in between the two lipid bilayers. The second compartment is formed by invaginations of the inner membrane known as **cristae**. They enclose the **cristae lumen**, which is separated from the intermembrane space by small narrow junctions. The cristae protrude into the innermost compartment of the mitochondria, the matrix [5–7].

During cellular respiration, organic molecules are oxidized in mitochondria by the **tricarboxylic acid cycle** and accompanying reactions. Electrons released from the cycle in the form of **NADH** and **FADH₂** are then used to drive the final step in respiratory energy conversion. This is fulfilled by the **OXPHOS** system, which produces **ATP**, the universal energy currency in all biological systems. The OXPHOS system comprises five large multisubunit complexes embedded in the cristae membrane. The first four complexes of the system (**complex I–IV**), which constitute the core of the **respiratory chain**, are involved in the transfer of electrons from NADH or FADH₂

Highlights

Recent high-resolution electron cryo-microscopy (cryo-EM) maps revealed detailed insights into the arrangement of the carbonic anhydrase (CA) module next to a ferredoxin subunit and a proton translocation channel of plant, algal, and protozoan mitochondrial complex I.

Complex I-anchored CA may promote the provision of protons at the inside of the inner mitochondrial membrane, thereby supporting oxidative phosphorylation (OXPHOS).

The cryoEM maps imply that a possible local pH difference between the active site of the CA module and the positive charge of a ferredoxin-bound single iron or iron–sulfur cluster facilitates the migration of protons to the entrance of a proton translocation channel at complex I.

In the context of early endosymbiosis with mitochondria lacking cristae invaginations that shield off high proton leakage, complex I-bound CAs might have ensured maintenance of OXPHOS.

¹Institute of Plant Genetics, Leibniz Universität Hannover, Herrenhäuser Str. 2, 30419 Hannover, Germany

²Department of Structural Biology, Max-Planck-Institute of Biophysics, Max-von-Laue-Straße 3, 60438 Frankfurt, Germany

*Correspondence: braun@genetik.uni-hannover.de (H.-P. Braun) and Niklas.Klusch@biophys.mpg.de (N. Klusch).

to molecular oxygen. This electron transfer is coupled to **proton** translocation from the matrix side across the inner membrane into the cristae lumen. The result is a proton-motive force created by an electrochemical gradient, which is characterized by an electrostatic ($\Delta\psi$) and chemical (ΔpH) component.

The proton-motive force finally drives **ATP synthase**, the complex V of the OXPHOS system, to produce ATP from ADP and inorganic phosphate [8]. The proton concentration in the **mitochondrial matrix** is comparatively lower but must be sufficient to enable proton export to the cristae lumen by the protein complexes of the respiratory chain. **CAs** can have an important role in adjusting the proton concentration in the mitochondrial matrix.

Carbonic anhydrases of the mitochondria

CAs catalyze the reversible hydration of carbon dioxide (CO_2) to bicarbonate (HCO_3^-) and a proton (H^+). In eukaryotes, they are present in several subcellular compartments and essential for various processes, including pH regulation, ion transport, and metabolic reactions [9,10]. CAs are divided into eight classes (α , β , γ , δ , ζ , η , θ , and ι), which are not evolutionarily related. Mammalian mitochondria include two α -type CAs (CA-VA and CA-VB; reviewed in [11]), while β -type CAs have been described for the mitochondria of algae and higher plants [12–14]. Besides their role in pH homeostasis of the mitochondrial matrix, further physiological functions were attributed to these enzymes, predominantly in the context of specific mitochondrial metabolic reactions.

In addition to β -type CAs, algal and plant mitochondria include γ -type CAs, which resemble the prototype γ CA from the archaeon *Methanosarcina thermophila* [15]. These γ CAs are abundant in algae and plants. Surprisingly, they were found to be attached to complex I of the respiratory chain [16,17], where they form a trimeric extra module that is absent in complex I of fungi and animals [18]. Likewise, protozoan complex I contains the γ -type CA module [19,20]. The physiological role of the complex I-anchored γ CAs is not yet clear. In plants, it has been suggested that conversion of CO_2 into bicarbonate in mitochondria contributes to the refixation of inorganic carbon in the Calvin–Benson cycle of chloroplasts [21–23]. An analogous system occurs in cyanobacteria, where the CupA protein, which is a CA of a special class, is associated with photosynthetic complex I and assumed to contribute to a CO_2 concentration mechanism supporting carbon assimilation [24]. Furthermore, the plant mitochondrial γ CA subunits are required for early steps of complex I assembly [25,26].

Complex I of the mitochondria

Complex I is an oxidoreductase that transfers electrons from NADH onto **ubiquinone** and simultaneously contributes to the formation of the proton gradient across the inner mitochondrial membrane [27,28]. Its L-shaped structure is defined by two connected extensive subcomplexes, which are referred to as the membrane and the peripheral arms. The membrane arm is embedded in the lipid bilayer of the inner mitochondrial membrane, while the peripheral arm projects into the mitochondrial matrix. The electron transfer reaction occurs in the peripheral arm, whereas the membrane arm translocates protons from the mitochondrial matrix to the mitochondrial cristae lumen. The mechanism that couples electron transfer to proton translocation is not yet fully understood, but appears to be based on structural constraints that have only recently been discovered. Starting from the ubiquinone-binding pocket at the base of the peripheral arm, a central aqueous passage traverses the entire membrane arm to its tip [29–32]. This aqueous passage is connected to the matrix side and to the cristae lumen by water half-channels created by subunits of the membrane arm, which are related to

Glossary

Alphaproteobacteria: a class of bacteria whose species are considered to be related to the ancestors of mitochondria.

ATP: general energy currency in cellular metabolism due to the release of free energy when ATP is hydrolyzed to ADP. The stoichiometric participation of ATP in a coupled reaction drives endergonic metabolic conversions.

ATP synthase: enzyme that uses the proton gradient across the inner mitochondrial membrane in eukaryotes or the plasma membrane of bacteria to produce ATP from ADP and inorganic phosphate.

Carbonic anhydrase (CA): zinc-containing enzyme that catalyzes the reversible conversion of CO_2 and H_2O into HCO_3^- and a proton (H^+).

Complex I: also known as the NADH dehydrogenase complex; the starting point of the respiratory chain. It oxidizes NADH and translocates protons across the inner mitochondrial membrane in eukaryotes or the plasma membrane in bacteria.

Cristae: invaginations of the inner mitochondrial membrane into the interior of mitochondria.

Cristae lumen: space within the invaginations of the inner mitochondrial membrane.

Cytosol: liquid phase of the cytoplasm within a cell that is separated from organelles by membranes.

Electron cryo-microscopy (cryo-EM): electron microscopy analysis of biological samples that are rapidly frozen in a thin layer of amorphous ice.

FADH₂: reduced form of the coenzyme FAD. It is involved in several redox reactions in biological systems.

Ferredoxin: iron-containing proteins that often are involved in electron transfer processes.

Intermembrane space: space between the outer and inner mitochondrial membrane.

Iron–sulfur clusters: cofactors of proteins comprising iron and inorganic sulfur that are arranged in different geometries. They are involved in electron transfer reactions.

Mitochondrial contact site and cristae organizing system (MICOS): forms narrow junctions between the intermembrane space and cristae lumen of mitochondria.

proton antiporters. It is assumed that protons are supplied to the central aqueous passage via the half-channels on the matrix side and released from the aqueous passage into the cristae lumen. Recent structures only showed open half-channels at the tip of the membrane arm. Additional half-channels that have been proposed along the membrane arm are closed off to the matrix and cristae lumen in currently available structures (reviewed in [27,28]). The mechanistic details of the redox-driven proton translocation at complex I are still under discussion [33–35].

The carbonic anhydrase module of mitochondrial complex I

Cryo-EM structures have shown how the trimeric carbonic anhydrase module is attached to complex I in plants and algae [36–39]. The module is tightly bound to the **ND2** subunit and some further accessory subunits of the membrane arm. In addition, one of the γ CA trimer subunits is connected to a **ferredoxin** that was recently discovered as part of a protein bridge, which links the two arms of complex I [38]. In the model plant arabidopsis (*Arabidopsis thaliana*), the ferredoxin is unusual, because it only contains a bound ion, likely iron, rather than an iron–sulfur cluster. At a resolution of 2 Å, the structure of the respiratory I+III₂ supercomplex from arabidopsis provided further insights into the CA module. The structure indicated a network of bound water molecules that surrounds a zinc ion needed for the CO₂/bicarbonate interconversion in one of the three catalytic sites of the trimer [40]. Based on these findings, it was concluded that this site of the γ CA module must be active because it exactly corresponds to that found in a bacterial γ -CA of the CamH-subtype [41,42]. The high-resolution structure also revealed a bound butyryl or crotonyl-CoA molecule at another site of the γ CA trimer [40]. The role of crotonyl-CoA might be to coordinate a CO₂ molecule, as has been shown in crotonyl-CoA carboxylase/reductases [43]. Crotonyl CoA within the CA module possibly creates a second active site, because the crotonyl group occupies the zinc binding site. The third putative catalytic site of the CA module is probably inactive.

The functional role of the carbonic anhydrase module of complex I

The ongoing resolution revolution in the field of cryo-EM now enables the structural determination of proteins at close to atomic detail [44–46]. This makes cryo-EM a suitable technique to gain structural and functional insights into membrane proteins, especially those that are difficult to crystallize. Above a resolution of ~2.5 Å, water molecules can be identified at defined positions in a cryo-EM map [47]. Localizing water molecules greatly promotes understanding of the proton transfer mechanism within a protein. Based on the cryo-EM structure of the arabidopsis respiratory I+III₂ supercomplex, numerous water molecules were found to be located in the central aqueous passage of the complex I membrane arm, the half-channels, and in the surrounding of the γ CA module. The structure suggests that protons are released by the CA module at a site close to the opening of a half-channel at the ND2 subunit on the matrix side of the membrane arm (Figure 1 [40]). An anticipated local pH difference between the active site at the γ CA module and ND2 promotes the migration of protons toward the ND2 opening. The positively charged iron ion of the ferredoxin bridge localized to the side of the half-channel opening may support entry of protons into the channel by repulsive electrostatic forces (Figure 1). As a consequence, the architecture and chemical constitution in this region of complex I may act as a funnel for the entrance of protons into the membrane arm.

The origin of the carbonic anhydrase module of complex I

Structural studies on *Tetrahymena* recently revealed that both CA module and the ferredoxin bridge also occur in protozoa [20,48–50] (Figure 2). *Tetrahymena* complex I-bound ferredoxin carries a Fe₂S₂ cluster instead of the Fe ion bound to ferredoxin of arabidopsis. However, in

Mitochondrial matrix: innermost compartment of mitochondria enclosed by the inner membrane.

NADH: reduced form of the coenzyme NAD. It serves as an electron carrier in biological systems and can be oxidized to NAD⁺.

ND2: subunit 2 of complex I; one of the three antiporter-like subunits located in the membrane arm of complex I.

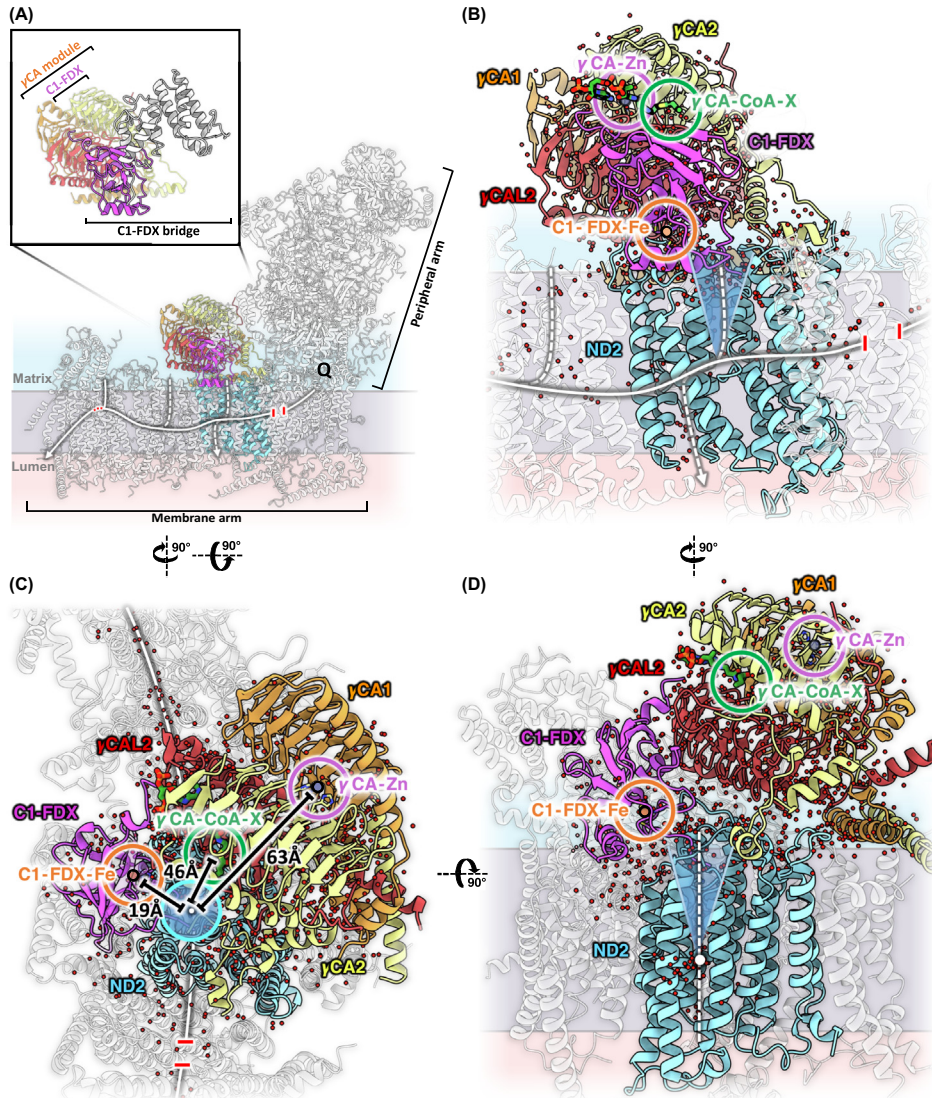
Oxidative phosphorylation (OXPHOS): oxygen-dependent phosphorylation of ADP into ATP. The process is part of cellular respiration. It occurs in mitochondria in eukaryotes.

Proton: cationic form of atomic hydrogen, also known as hydron (H⁺). Note that free protons will not occur in aqueous solutions but are bound to water molecules and other polar compounds.

Respiratory chain: chain of enzyme complexes within the cristae membrane or the plasma membrane of bacteria that transfers electrons from NADH or FADH₂ to molecular oxygen, thereby translocating protons across the membrane and creating a proton gradient.

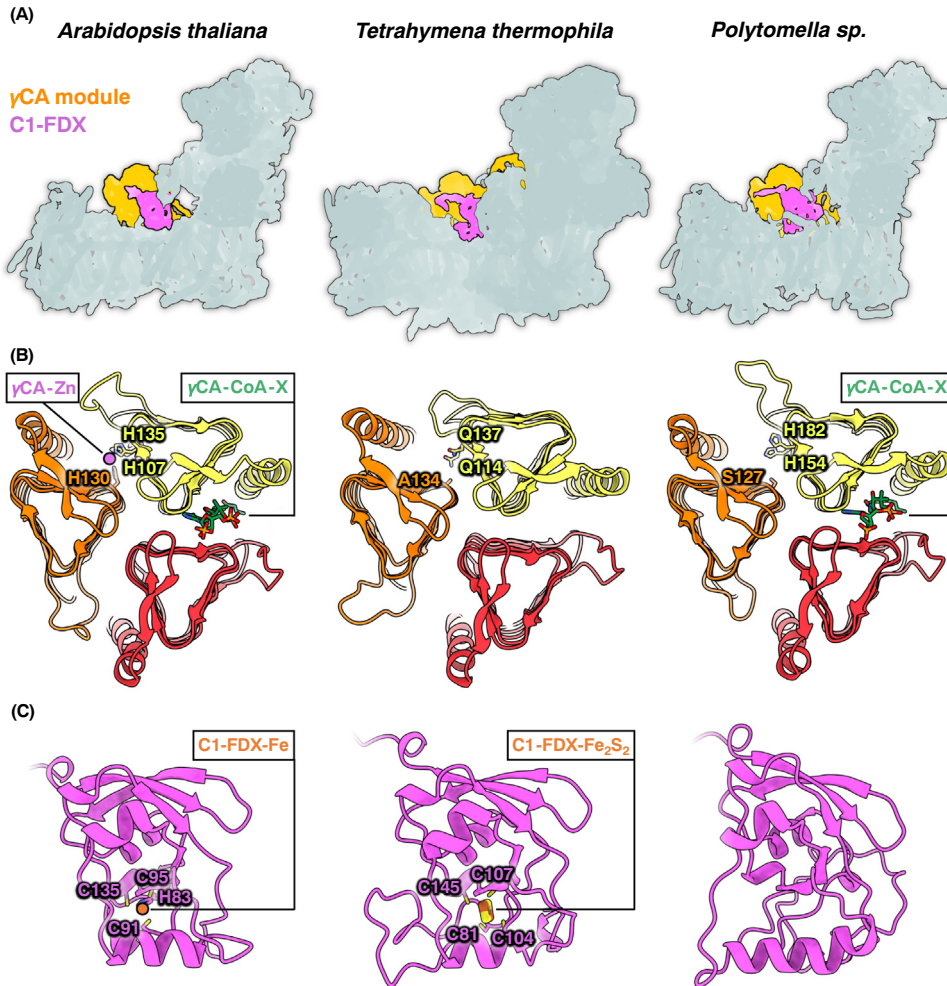
Tricarboxylic acid cycle: also known as the citric acid or Krebs cycle; located in the mitochondrial matrix and the lumen of bacterial cells. It oxidizes an acetyl-group into two molecules of CO₂. Electrons that become available are provided to the oxidative phosphorylation system via NADH and FADH₂.

Ubiquinone: a cofactor involved in electron transfer between enzyme complexes of the respiratory chain. It is considered to play an important role in the coupling of redox reactions with proton translocation at complexes I and III.



Trends in Plant Science

Figure 1. Topological arrangement of ND2, the ferredoxin subunit C1-FDX, and the γ -carbonic anhydrase module (γ CA) in *Arabidopsis thaliana* (arabidopsis) mitochondrial complex I. (A) Overview. Complex I is defined by a peripheral and membrane arm. An aqueous passage (white line) traverses the entire membrane arm from the ubiquinone-binding site (Q) to its tip. In the resting state of complex I, the passage is interrupted (red bars and red dashed line). Putative water half-channels connecting the aqueous passage with the matrix or the cristae lumen are indicated by dashed white lines. The ND2 subunit (cyan) forms an integral part of the membrane arm of complex I. C1-FDX (magenta) and the subunits of the γ CA module (yellow, orange, and red) are attached to ND2 on the matrix side of the membrane arm. Inset: Arrangement of the γ CA module and the C1-FDX bridge connecting the two arms of complex I. (B) Enlarged view. The active catalytic site of the γ CA module with bound zinc for CO_2 /bicarbonate interconversion (pink circle) and a second possible catalytic site with bound CoA (green circle) are highlighted. The ion of C1-FDX, likely to be iron, is marked by a circle in orange. Red dots indicate water molecules. The putative half channel to the matrix at ND2 is highlighted in blue. (C,D) Same as (B), but seen from the matrix side (C) and along the membrane arm from the Q-binding site (D). Distances between the putative half channel opening and C1-FDX-Fe (19 Å), bound CoA (46 Å) and zinc (63 Å) are indicated in (C). Structural coordinates are from Protein Data Bank ID: 8BPX.



Trends in Plant Science

Figure 2. The complex I-anchored γ -carbonic anhydrase (CA) module and ferredoxin subunit C1-FDX in plants, protozoa, and algae. (A) Cartoon overview of the mitochondrial complex I structure in *Arabidopsis thaliana* (arabidopsis), *Tetrahymena thermophila*, and *Polytomella* sp. The complex I-associated γ CA module and the ferredoxin subunit (C1-FDX) are highlighted in orange and magenta. (B) Cross-section of the trimeric γ CA module at the level of the catalytic sites for the three species (ribbon diagram). In arabidopsis, a zinc ion (γ CA-Zn, pink) for CO₂/bicarbonate interconversion is coordinated by three histidine sidechains in one of the catalytic sites. A zinc ion is missing in the γ CA module of *Tetrahymena* and *Polytomella* complex I, possibly representing an inactive γ CA trimer in these two species. In arabidopsis and *Polytomella*, a coenzyme A (γ CA-CoA-X, green) is bound in an additional catalytic site, suggesting that it coordinates a CO₂ molecule and creates another active center. (C) Ribbon diagram of the C1-FDX subunit for the three species. In arabidopsis, a single metal ion, possibly iron (C1-FDX-Fe), is coordinated by one histidine and three cysteine sidechains. In *Tetrahymena*, four cysteines coordinate an Fe₂S₂ cluster (C1-FDX-Fe₂S₂). In *Polytomella*, the catalytic site of C1-FDX is unoccupied. Electron cryo-microscopy maps and atomic structures: Protein Data Bank (PDB) ID 8BEF and Electron Microscopy Data Bank (EMDB) ID 16168 for arabidopsis; PDB ID 7TGH and EMDB ID 25882 for *Tetrahymena*; and PDB ID 7AR9 and EMDB ID 11880 for *Polytomella*.

the alga *Polytomella*, the ferredoxin possibly lost its capability to bind a cofactor [38]. The CA activity of the γ CA modules in alga and protozoans is not clear from the structural data. However, it can be concluded that the CA module and the ferredoxin bridge represent original features of eukaryotic complex I, likely present in the Last Eukaryotic Common Ancestor

(LECA). Mitochondrial complex I has evolved from bacterial complex I; however, this has a much simpler structure and comprises only 14–17 subunits. During mitochondrial evolution, the number of complex I subunits has greatly increased to ensure its functioning in the context of endosymbiosis [51]. We speculate that the attachment of the CA module to complex I in early mitochondria provided functional advantages. Proton gradients at membranes are generally affected by proton loss. In case of mitochondria, protons can leak across the porous outer mitochondrial membrane into the cytosol. We suggest that the attachment of CAs to complex I in close proximity to the entrance of a proton half-channel supported the maintenance of OXPHOS in the context of early endosymbiosis. During later stages of evolution, the ultrastructure of mitochondria evolved considerably, supporting OXPHOS by other means. Cristae, deep invaginations of the inner mitochondrial membrane, emerged, which are likely to have evolved from more simple intracytoplasmic membranes present in bacteria [52]. The cristae significantly increase the surface area of the inner membrane and allow relocation of the OXPHOS complexes in compartments away from the leaky outer porous mitochondrial bilayer. As a result, the development of the cristae likely had a stabilizing effect on the proton gradient across the inner mitochondrial membrane [53]. In addition, the **'mitochondrial contact site and cristae organizing system' (MICOS)** evolved. This protein complex supports the formation of narrow cristae junctions, which partially demarcate the lumen of the cristae from the mitochondrial intermembrane space and mediate physical interactions of the outer and inner mitochondrial membrane [54]. We suggest that this ultrastructure of mitochondria made the anchoring of CAs in complex I dispensable and, consequently, the γ CA module was lost from the mitochondria of animals and fungi. The reason why the original configuration has been preserved in the green lineage (Viridiplantae) requires further investigation, but it might be linked to the proposed role of the γ CA module in the re-assimilation of mitochondrial CO_2 by the Calvin–Benson cycle in chloroplasts [21–23]. Furthermore, the respiratory chain of plant mitochondria is known to include numerous non-proton pumping alternative oxidoreductases, which might also have contributed to specific routes in evolution.

Concluding remarks and future perspectives

Based on the new structures obtained by cryo-EM, we propose that the CAs bound to mitochondrial complex I in protozoans, algae, and plants are relevant for the maintenance of the mitochondrial proton gradient and, thus, for OXPHOS (Figure 3, Key figure). Under the alkaline conditions in the mitochondrial matrix, the γ CA promotes HCO_3^- and H^+ formation. Thus, protons can be provided for translocation across the membrane arm. Proton migration from the active site of the complex I-anchored γ CA module toward the nearby half-channel at subunit ND2 would be enabled by an anticipated local pH difference. Proton migration toward the ND2 half-channel entrance would further be assisted by a positive repulsive electrostatic force surrounding the iron ion or iron–sulfur cluster of the ferredoxin. In the future, structural investigations of complex I under substrate turnover and under the condition of an existing proton gradient could reveal whether the ND2 half-channels toward the matrix and luminal side are indeed pathways for proton translocation (see Outstanding questions). To test our hypothesis that the γ CA module contributes to maintaining a proton gradient across the inner mitochondrial membrane, targeted gene modifications can be used, affecting, for example, the amino acid positions of the γ CA subunits relevant for Zn^{2+} coordination [55]. The implied local pH difference between the active site of the γ CA module and the entrance of the half-channel at ND2 on the matrix side can be tested by molecular pH sensors. Using this experimental approach, local pH gradients of up to 0.4 units were monitored at the surface of the cristae lumen side of the inner mitochondrial membrane [56,57]. Furthermore, activities of the γ CA module in protozoa, algae, and plants have yet to be characterized. We suggest a general role of mitochondrial CAs for maintenance of OXPHOS in eukaryotes.

Outstanding questions

Are the CA and ferredoxin subunits also part of mitochondrial complex I in clades other than plants, green algae, and protozoa?

Is the CA module of mitochondrial complex I active in all clades?

Does inactivation of the active site(s) of the CA module affect the proton translocation rate of plant complex I at defined physiological conditions?

Is there a local difference in pH between the active site(s) of the CA module and the opening of the water half channel on the matrix-side at ND2?

Is the water half-channel at the matrix-side of ND2 used for proton translocation and, assuming that is the case, how is this translocation regulated?

How is oxidoreduction in the peripheral arm of complex I energetically coupled to proton translocation across the inner mitochondrial membrane by its membrane arm?

Does conversion of mitochondrial CO_2 into bicarbonate promote its refixation by the Calvin–Benson cycle in the chloroplasts?

Key figure

The γ -carbonic anhydrase (CA) module of plant complex I provides protons for translocation across the inner mitochondrial membrane at complex I

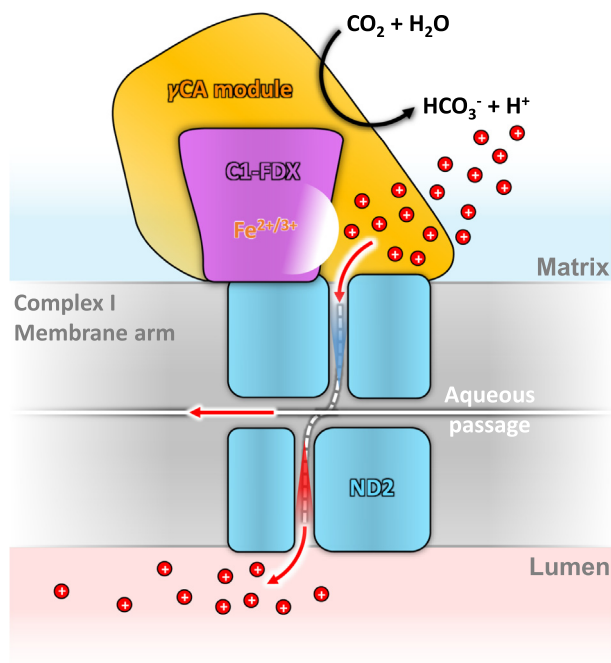
**Trends in Plant Science**

Figure 3. Cartoon overview of the γ CA module (orange), the ferredoxin subunit C1-FDX (magenta), and ND2 (cyan) arrangement in the complex I membrane arm (gray) as seen along the inner mitochondrial lipid bilayer separating the mitochondrial matrix and the cristae lumen. Under alkalinizing conditions, the catalytic reaction of the γ CA shifts to bicarbonate (HCO_3^-) and proton (H^+) production. An anticipated local pH difference between the active site at the γ CA module and ND2, as well as a positive repulsive electrostatic force surrounding the iron ion of the ferredoxin (white half sphere) have a promoting effect on the migration of protons (red dots) in the direction of the ND2 opening. Possible proton paths are indicated by red arrows. Protons can travel either along the aqueous passage in the center of the membrane arm or directly into the cristae lumen through a possible water half channel at the ND2 site.

Acknowledgments

We thank Werner Kühlbrandt and Jennifer Senkler for critically reading the manuscript. The research in our laboratories is funded by the Max Planck Society (N.K.) and the Deutsche Forschungsgemeinschaft (grant INST 187/791-1 FUGG to H-P.B.).

Declaration of interests

None declared by authors.

References

1. Siekevitz, P. (1957) Powerhouse of the cell. *Sci. Am.* 197, 131–144
2. Schatz, G. (1995) Mitochondria: beyond oxidative phosphorylation. *Biochim. Biophys. Acta* 1271, 123–126
3. Sagan, L. (1967) On the origin of mitosing cells. *J. Theor. Biol.* 14, 255–274
4. Martin, W. and Mentel, M. (2010) The origin of mitochondria. *Nat. Educ.* 3, 58
5. Palade, G.E. (1952) The fine structure of mitochondria. *Anat. Rec.* 114, 427–451
6. Frey, T.G. and Mannella, C.A. (2000) The internal structure of mitochondria. *Trends Biochem. Sci.* 25, 319–324

7. Ježek, P. *et al.* (2023) Mitochondrial cristae morphology reflecting metabolism, superoxide formation, redox homeostasis, and pathology. *Antioxid. Redox Signal.* Published online April 11, 2023. <https://doi.org/10.1089/ars.2022.0173>
8. Mitchell, P. (1961) Coupling of phosphorylation to electron and hydrogen transfer by a chemi-osmotic type of mechanism. *Nature* 191, 144–148
9. Supuran, C.T. (2016) Structure and function of carbonic anhydrases. *Biochem. J.* 473, 2023–2032
10. Nocentini, A. *et al.* (2021) An overview on the recently discovered iota-carbonic anhydrases. *J. Enzyme Inhib. Med. Chem.* 36, 1988–1995
11. Aspatwar, A. *et al.* (2023) Mitochondrial carbonic anhydrase VA and VB: properties and roles in health and disease. *J. Physiol.* 601, 257–274
12. Eriksson, M. *et al.* (1996) Discovery of an algal mitochondrial carbonic anhydrase: molecular cloning and characterization of a low-CO₂-induced polypeptide in *Chlamydomonas reinhardtii*. *Proc. Natl. Acad. Sci. U. S. A.* 93, 12031–12034
13. Giordano, M. *et al.* (2003) An anaplerotic role for mitochondrial carbonic anhydrase in *Chlamydomonas reinhardtii*. *Plant Physiol.* 132, 2126–2134
14. Fabre, N. *et al.* (2007) Characterization and expression analysis of genes encoding alpha and beta carbonic anhydrases in *Arabidopsis*. *Plant Cell Environ.* 30, 617–629
15. Alber, B.E. and Ferry, J.G. (1994) A carbonic anhydrase from the archaeon *Methanosarcina thermophila*. *Proc. Natl. Acad. Sci. U. S. A.* 91, 6909–6913
16. Parisi, G. *et al.* (2004) Gamma carbonic anhydrases in plant mitochondria. *Plant Mol. Biol.* 55, 193–207
17. Cardol, P. *et al.* (2005) The mitochondrial oxidative phosphorylation proteome of *Chlamydomonas reinhardtii* deduced from the Genome Sequencing Project. *Plant Physiol.* 137, 447–459
18. Sunderhaus, S. *et al.* (2006) Carbonic anhydrase subunits form a matrix-exposed domain attached to the membrane arm of mitochondrial complex I in plants. *J. Biol. Chem.* 281, 6482–6488
19. Gawryluk, R.M. and Gray, M.W. (2010) Evidence for an early evolutionary emergence of gamma-type carbonic anhydrases as components of mitochondrial respiratory complex I. *BMC Evol. Biol.* 10, 176
20. Zhou, L. *et al.* (2022) Structures of *Tetrahymena*'s respiratory chain reveal the diversity of eukaryotic core metabolism. *Science* 376, 831–839
21. Zabaleta, E. *et al.* (2012) A basal carbon concentrating mechanism in plants? *Plant Sci.* 187, 97–104
22. Soto, D. *et al.* (2015) Functional characterization of mutants affected in the carbonic anhydrase domain of the respiratory complex I in *Arabidopsis thaliana*. *Plant J.* 83, 831–844
23. Fromm, S. *et al.* (2016) The carbonic anhydrase domain of plant mitochondrial complex I. *Physiol. Plant.* 157, 289–296
24. Schuller, J.M. *et al.* (2020) Redox-coupled proton pumping drives carbon concentration in the photosynthetic complex I. *Nat. Commun.* 11, 494
25. Perales, M. *et al.* (2005) Disruption of a nuclear gene encoding a mitochondrial gamma carbonic anhydrase reduces complex I and supercomplex I + III₂ levels and alters mitochondrial physiology in *Arabidopsis*. *J. Mol. Biol.* 350, 263–277
26. Ligas, J. *et al.* (2019) The assembly pathway of complex I in *Arabidopsis thaliana*. *Plant J.* 97, 447–459
27. Parey, K. *et al.* (2020) Respiratory complex I - structure, mechanism and evolution. *Curr. Opin. Struct. Biol.* 63, 1–9
28. Kampjüt, D. and Sazanov, L.A. (2022) Structure of respiratory complex I – an emerging blueprint for the mechanism. *Curr. Opin. Struct. Biol.* 74, 102350
29. Kampjüt, D. and Sazanov, L.A. (2020) The coupling mechanism of mammalian respiratory complex I. *Science* 370, eabc4209
30. Grba, D.N. and Hirst, J. (2020) Mitochondrial complex I structure reveals ordered water molecules for catalysis and proton translocation. *Nat. Struct. Mol. Biol.* 27, 892–900
31. Parey, K. *et al.* (2021) High-resolution structure and dynamics of mitochondrial complex I—Insights into the proton pumping mechanism. *Sci. Adv.* 7, eabj3221
32. Laube, E. *et al.* (2022) Conformational changes in mitochondrial complex I of the thermophilic eukaryote *Chaetomium thermophilum*. *Sci. Adv.* 8, eadc9952
33. Kravchuk, V. *et al.* (2022) A universal coupling mechanism of respiratory complex I. *Nature* 609, 808–814
34. Sazanov, L.A. (2023) From the 'black box' to 'domino effect' mechanism: what have we learned from the structures of respiratory complex I. *Biochem. J.* 480, 319–333
35. Gu, J. *et al.* (2022) The coupling mechanism of mammalian mitochondrial complex I. *Nat. Struct. Mol. Biol.* 29, 172–182
36. Soufari, H. *et al.* (2020) Specific features and assembly of the plant mitochondrial complex I revealed by cryo-EM. *Nat. Commun.* 11, 5195
37. Maldonado, M. *et al.* (2020) Atomic structure of a mitochondrial complex I intermediate from vascular plants. *Elife* 9, e56664
38. Klusch, N. *et al.* (2021) A ferredoxin bridge connects the two arms of plant mitochondrial complex I. *Plant Cell* 33, 2072–2091
39. Maldonado, M. *et al.* (2023) Plant-specific features of respiratory supercomplex I + III₂ from *Vigna radiata*. *Nat. Plants* 9, 157–168
40. Klusch, N. *et al.* (2023) Cryo-EM structure of the respiratory I + III₂ supercomplex from *Arabidopsis thaliana* at 2 Å resolution. *Nat. Plants* 9, 142–156
41. Jeyakanthan, J. *et al.* (2008) Observation of a calcium-binding site in the gamma-class carbonic anhydrase from *Pyrococcus horikoshii*. *Acta Crystallogr. D Biol. Crystallogr.* 64, 1012–1019
42. Ferry, J.G. (2010) The gamma class of carbonic anhydrases. *Biochim. Biophys. Acta* 1804, 374–381
43. Wilson, M.C. and Moore, B.S. (2012) Beyond ethylmalonyl-CoA: the functional role of crotonyl-CoA carboxylase/reductase homologs in expanding polyketide diversity. *Nat. Prod. Rep.* 29, 72–86
44. Kühlbrandt, W. (2014) Biochemistry. The resolution revolution. *Science* 343, 1443–1444
45. Nakane, T. *et al.* (2020) Single-particle cryo-EM at atomic resolution. *Nature* 587, 152–156
46. Yip, K.M. *et al.* (2020) Atomic-resolution protein structure determination by cryo-EM. *Nature* 587, 157–161
47. Beckers, M. *et al.* (2021) Structural interpretation of cryo-EM image reconstructions. *Prog. Biophys. Mol. Biol.* 160, 26–36
48. Huynen, M.A. and Elurbe, D.M. (2022) Mitochondrial complex complexification. *Science* 376, 794–795
49. Mühleip, A. *et al.* (2023) Structural basis of mitochondrial membrane bending by the I-II-III₂-IV₂ supercomplex. *Nature* 615, 934–938
50. Han, F. *et al.* (2023) Structures of *Tetrahymena thermophila* respiratory megacomplexes on the tubular mitochondrial cristae. *Nat. Commun.* 14, 2542
51. Padavani, A. *et al.* (2021) The mysterious multitude: structural perspective on the accessory subunits of respiratory complex I. *Front. Mol. Biosci.* 8, 798353
52. Muñoz-Gómez, S.A. *et al.* (2017) The origin of mitochondrial cristae from Alphaproteobacteria. *Mol. Biol. Evol.* 34, 943–956
53. Joubert, F. and Puff, N. (2021) Mitochondrial cristae architecture and functions: lessons from minimal model systems. *Membranes (Basel)* 11, 465
54. Rampelt, H. *et al.* (2017) Role of the mitochondrial contact site and cristae organizing system in membrane architecture and dynamics. *Biochim. Biophys. Acta Mol. Cell Res.* 1864, 737–746
55. Fromm, S. *et al.* (2016) Mitochondrial gamma carbonic anhydrases are required for complex I assembly and plant reproductive development. *New Phytol.* 211, 194–207
56. Rieger, B. *et al.* (2014) Lateral pH gradient between OXPHOS complex IV and F₀F₁ ATP-synthase in folded mitochondrial membranes. *Nat. Commun.* 5, 3103
57. Rieger, B. *et al.* (2021) Mitochondrial F₁F₀ ATP synthase determines the local proton motive force at cristae rims. *EMBO Rep.* 22, e52727